

# Design and Development of High Power Rectangular Ka-Band WR-51 Waveguide Pressure Window for Satellite Testing Applications

Karri V R Dinesh Kumar Reddy<sup>1</sup>, Md.Tosicul Wara<sup>2</sup>, Shaji V Sebastian<sup>3</sup>,  
T. Ramesh Babu Reddy<sup>4</sup>, K. Chandrasekharam<sup>5</sup>, Usha Bhandiwad<sup>6</sup>

GEOSAT RF & Payload Checkout Division-1, Spacecraft Checkout Group, U R Rao Satellite Center, Bangalore-560017, India

**Abstract:** An analytical approach is presented to achieve the design and development of High power RF Waveguide pressure window. The theoretical calculations are carried out in MATLAB and the simulations are carried out in High frequency structure simulator. This paper presents the detailed developmental work for realization of RF waveguide pressure windows used for Satellite testing applications. In this paper, the design is carried out in the Ka-band frequency with inductive type of iris. Alumina is chosen as dielectric for its high power handling capacity. Silicone gasket is used for attachment of substrate to flange and for providing required level of vacuum sealing. Detailed process of Test and Qualification of Pressure window has been presented in this paper. Waveguide pressure windows have been developed at payload downlink frequencies in Ka-band and are being used for characterisation of Communication payload.

**Keywords:** High Frequency Structure Simulator (HFSS), IRIS matching, Pressure Window, Radio Frequency, Scattering parameters, Thermal-vacuum testing, Vector network analyzer (VNA)

## 1. Introduction

A wave guide pressure window is a passive device which is used to isolate high vacuum and ambient condition while allowing the RF electromagnetic energy transmission. Pressure window shall act as a mechanical gate for pressure, with electrically transparency towards microwave transmission. Design constraints of Pressure window are good Insertion loss and Return loss, Wider bandwidth, High thermal capacity for the dielectric to withstand high power transmissions and very low leak rate to maintain vacuum conditions. Figure 1 shows the waveguide pressure window designed in Ka band.

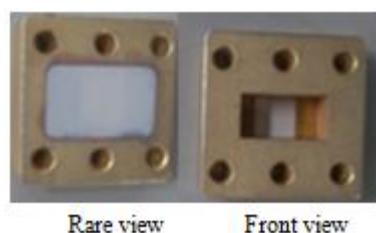


**Figure 1:** Ka- Band WR-51 waveguide pressure window

Pressure window is mechanical alumina substrate which are having following features:

- Alumina substrate is chosen as dielectric because of its high power handling capability
- Alumina materials are thermally equivalent for use in high temperature situation
- Pressure windows are used where it is desirable to environmentally isolate a section of transmission line
- It is electrically transparent to microwave transmission medium and mechanically a gate for pressure
- These pressure windows are designed by using HFSS software

Each pressure window is characterised for electrical and environmental performance. It is used at the interface of thermo-vacuum chamber and for differentiating vacuum and ambient conditions existing on either side of the chamber.

Choice of material is a challenging task while designing a waveguide pressure window as it is used in high power and in high vacuum environment. In this paper, the pressure window is designed using Alumina (dielectric constant = 9.8) owing to its high mechanical strength, low cost and ease of fabrication. Inductive iris matching technique is used for impedance matching and the design equations are coded in MATLAB for retrieving the design parameters to meet the specifications in Ka-band frequencies. Figure 2 shows the Alumina dielectric fabricated with the dimensions calculated using inductive iris matching technique.



**Figure 2:** Alumina Dielectric with inductive iris matching

As the technology advances, the RF power levels in Satellite transponders are increasing and with increase in power level there is a requirement in usage of waveguides as the transmission medium. Rectangular waveguides are hollow tubes that allow electromagnetic transmission with low loss and high power handling capacities at higher frequencies. For interfacing vacuum environment of satellite to the general laboratory conditions during thermal-vacuum testing of satellite, waveguide pressure windows are essential. Figure 3 shows the flow of RF signal transmitted through waveguide from satellite located inside thermal-vacuum chamber to the coupler load combination present inside lab which is maintained at ambient condition.

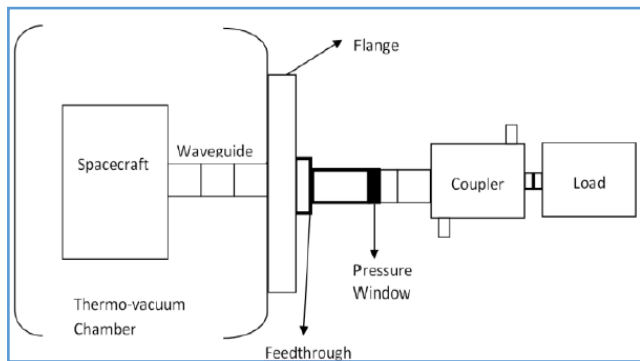


Figure 3: Interfacing between thermal-vacuum chamber and laboratory conditions

The desired specifications of a waveguide pressure window are the following:

- High dielectric breakdown voltage
- Low insertion loss
- Good return loss
- Wider bandwidth
- High thermal capacity for the dielectric to withstand high power transmissions
- Matched dimensions
- Very low leak rate to maintain vacuum condition

The target specifications of the indigenously developed Ka-band WR-51 waveguide pressure window are shown in Table 1

Table 1: Target Specification

SN	Parameters	Specified values
1	Operating Frequency Range	19.7 GHz-20.7 GHz
2	Bandwidth	1 GHz
3	Insertion Loss	≤ 0.4 dB
4	Return Loss (at the input and output)	≥ 15dB over the bandwidth
5	Maximum Power Handling	200wattCW Power
6	Pressure Hold (Maximum Differential Pressure)	2Atmosphere for 24 hours
7	Leak rate	≤ 1 x 10 <sup>-8</sup> tor.litre/sec
8	Operating Temperature Range	-20 Degree C to 100 Degree C (maximum)

The rest of the paper is organized as follows. In Section 2, detailed Analytical approach with all the theoretical equations, MATLAB coding and simulation test results carried out in HFSS are given. In Section 3, design process flow and fabrication details are given. In section 4, test and qualification process flow is described and the test results are given. Finally, in section 5 we discuss the application of this waveguide pressure window in satellite testing.

## 2. Waveguide Pressure Window Design

In this section, the basic detailed analytical approach, theoretical calculation of iris dimensions and HFSS simulations are discussed.

### 2.1 Basic Principle

Pressure window is a metallic flange filled with dielectric. The dielectric slab is placed in the hollow waveguide, due to

which there exists a mismatch in waveguide impedance. To counter the impedance mismatch created by dielectric slab, an iris matching technique is required to nullify the mismatch. There are different types of iris matching techniques like inductive iris matching, capacitive iris matching and the combination of both. Each iris matching has its own advantages and disadvantages. Here, inductive iris matching technique is used for better power handling capacity. Figure 4 shows the inductive iris matching in a waveguide.

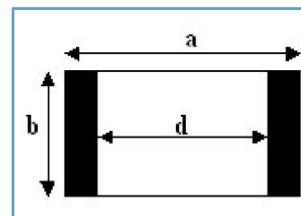


Figure 4: Inductive iris matching in a rectangular waveguide, a is the broad and b is narrow dimension of waveguide, d is iris width

An iris is an aperture in a thin metal that extends transversely across the waveguide. In inductive iris, the aperture extends completely across the waveguide with the edges being parallel to the electric field and transverse to the magnetic field. There are two types of inductive iris matching, namely the symmetrical iris and the asymmetrical iris. In our design, symmetrical inductive iris matching is used.

#### 2.1.1 Impedance Matching by Inductive Waveguide Iris

The placement of Alumina slab in the air-filled rectangular waveguide will give rise to an additional capacitive shunt reactance (negative reactance). The use of inductive waveguide iris at the location of the Alumina slab will give rise to an additional inductive shunt reactance (positive reactance). When the magnitudes of both these reactances are equal, both will nullify each other and thereby will improve the impedance matching by ensuring that the characteristic wave impedance of the air-filled rectangular waveguide is always equal to the intrinsic impedance of the air dielectric within the waveguide.

Theoretical equations for reactances are given below.

- a) The magnitude of additional inductive shunt reactance,  $X_L$  due to the inductive iris is given as [1,2]

$$\frac{X_L}{Z_0} = \frac{a}{\lambda_g} \tan^2 \left( \frac{\pi d}{2a} \right) \left\{ 1 + \frac{3}{4} \left( \frac{1}{\sqrt{1 - \left( \frac{2a}{3\lambda} \right)^2}} - 1 \right) \sin^2 \left( \frac{\pi d}{a} \right) + 2a\lambda_1 - 4\pi E\alpha - \beta^2 F\alpha\alpha^2 E\beta - \alpha^2 E\beta\beta^2 - 112 \sin^2 \pi d a \right\} \quad (1)$$

where,

$$\alpha = \sin \left( \frac{\pi d}{2a} \right) \text{ and } \beta = \cos \left( \frac{\pi d}{2a} \right)$$

$E(\alpha)$  and  $E(\beta)$  are the elliptical integrals of 2<sup>nd</sup> kind,  $F(\alpha)$  is the elliptical integral of 1st kind

$$\lambda_g = \text{guided wavelength of rectangular waveguide}$$

$$\lambda = \text{free space wavelength,}$$

- a = broad side waveguide dimension
- b = narrow side waveguide dimension
- d = inductive iris width
- Z<sub>0</sub> = intrinsic of the air-dielectric (= 377 ohms)

b) For a thin sheet like dielectric slab, the magnitude of the capacitive shunt reactance, X<sub>C</sub> be written as [3]

$$\frac{X_C}{Z_0} = \frac{2\pi t \lambda_c^2}{\lambda_g(\lambda_c^2 - \lambda^2)} (K_e - 1) \quad (2)$$

where,

- λ<sub>g</sub> = guided wavelength of rectangular waveguide
- λ<sub>c</sub> = cut-off wavelength of rectangular waveguide
- λ = free space wavelength
- t = thickness of the thin sheet like dielectric slab
- K<sub>e</sub> = dielectric constant (real part) of the slab material
- Z<sub>0</sub> = intrinsic of the air-dielectric (= 377 ohms)

### 2.1.2 Computation of Inductive Iris Width

Here, the impedance mismatch created by Alumina dielectric slab is nullified by inductive iris matching. Hence, by equating the Equations (1) and (2), the iris width, d for Alumina dielectric slab placed across the rectangular waveguide WR-51 could be calculated.

For WR-51 Rectangular waveguide[4],

- a = Broadside waveguide dimension = 12.95mm
- b = narrow side waveguide dimension = 6.47mm
- f<sub>c</sub> = cut-off frequency (=c/λ<sub>c</sub>) = 20.2 GHz

For Alumina dielectric slab,

- t = dielectric slab thickness = 10 mil
- K<sub>e</sub> = dielectric constant (real part) = 9.6

Consequently, the iris width (d) was computed as 6.27 mm using MATLAB program [5].

## 2.2 HFSS Simulations and Analysis

Using the above stated design parameters, a simulation is carried out in High Frequency Structure Simulator (HFSS) for a bandwidth of 1GHz with a center frequency of 20.2GHz. The material for dielectric slab is chosen to be Alumina due to its low loss properties. HFSS Simulation design is shown in Figure5.

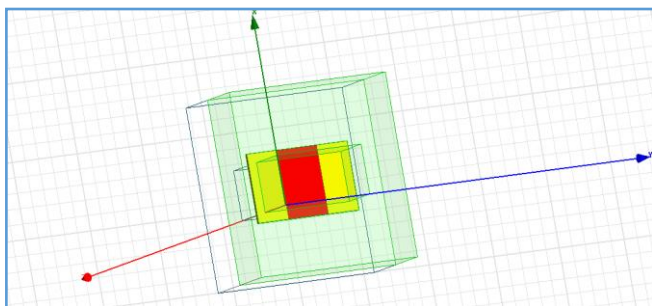


Figure 5: HFSS design simulation of Ka-band WR-51 waveguide pressure window

Then parametric analysis using HFSS was carried out to get the actual dimensions. A comparison of the S parameter characteristics over the bandwidth obtained from various

dielectric constants is carried out as the material properties change with temperature. Their width is chosen by varying the dielectric constant considering the change in temperature. The material has a dielectric constant (or relative permittivity) of 9.6 and a loss tangent of 0.008. HFSS simulations are carried out by varying the dielectric constant at the theoretically calculated iris width (= 6.27 mm). It is observed that with increase in dielectric constant, the operating frequency range (bandwidth) of pressure window is shifting towards lower side. Simulation results are provided in the Table 2.

Table 2: Dielectric constant versus operating frequency range

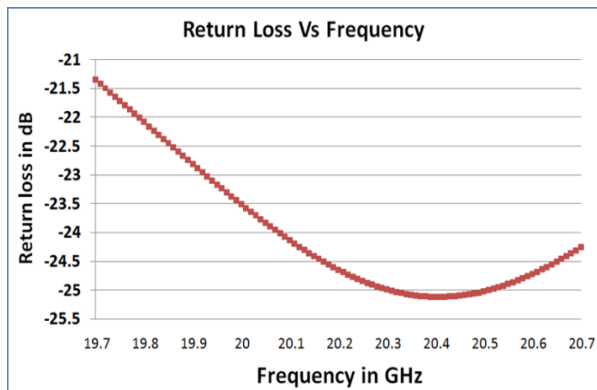
Dielectric constant	Operating Frequency Range
9.4	19.2-21.2 GHz
9.5	19-21 GHz
<b>9.6</b>	<b>18.8-20.8 GHz</b>
9.7	18.7-20.7 GHz
9.8	18.4-20.6 GHz
9.9	18.6-20.6 GHz
10	18.4-20.3 GHz

Considering the above observations, simulations were carried out by changing the parametric value of iris width to achieve the target operating frequency range of **19.7 GHz to 20.7 GHz** at the maximum possible dielectric constant. Here, the dielectric constant of 10 (maximum possible) is considered and the simulations were carried out for various iris widths. The Simulation results are shown in Table 3.

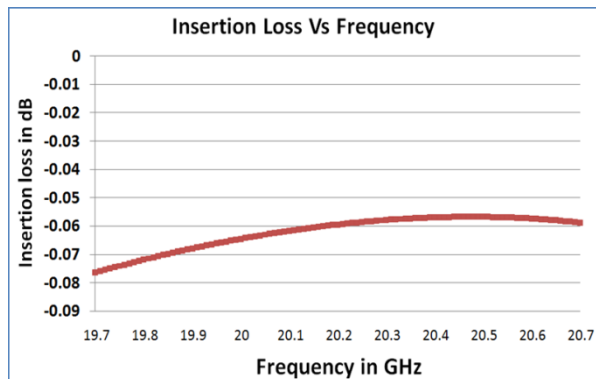
Table 3: Inductive iris width versus operating frequency range at dielectric constant, 10

Iris width	Operating Frequency Range
6.27	18.6-20.55 GHz
6.28	18.7-20.65 GHz
6.29	18.7-20.65 GHz
6.3	18.85-20.7 GHz
6.31	18.9-20.8 GHz
6.32	19-20.85 GHz
6.33	19.05-20.85 GHz
<b>6.34</b>	<b>19.15-20.90 GHz</b>
6.35	19.2-21.05 GHz
6.36	19.2-21.05 GHz
6.37	19.35-21.15 GHz
6.38	19.4-21.3 GHz
6.39	19.4-21.3 GHz
6.40	19.5-21.3 GHz

Considering the analytical results as shown in Tables 2 and 3, it is observed that at an iris width of 6.34mm, target operating frequency range of **19.7 GHz to 20.7 GHz** is always achieved for change in dielectric constant in the range of 9.4 to 10. The HFSS simulation's S parameter results for dielectric constant of 9.6 (nominal value) and iris width of 6.34 mm (analytical value) are shown in Figures 6(a) and 6(b).



(a)



(b)

**Figure 6:** (a)Return loss vs frequency plot of WR-51 pressure window at IRIS width 6.34 mm and dielectric constant 9.6 (b) Insertion loss vs frequency plot of WR-51 pressure window at IRIS width 6.34mm and dielectric constant 9.6

The above mentioned target specifications are achieved and the detailed test and evaluation plan and test results are shown in section 4.

### 3. Pressure Window Design Process Flow

Pressure window design process is discussed in this section. Initially, theoretical parameters are obtained from the available literature and with the available parameters, a design is created in High frequency structure simulator (HFSS)[6] and simulations are carried out. After successfully obtaining the parametric results and on comparison with the theoretical parameters, a dielectric is fabricated using thin film techniques with the dimensions obtained from HFSS simulation. For holding this dielectric slab, a pressure window holder is fabricated. Now, for bonding the dielectric slab on pressure window holder, RTV S 691 bonding material is used as an adhesive. This is used as bonding material because of its material properties like electrical conductivity, thermal conductivity and outgassing. Post bonding, detailed test and qualification is carried out and the details of testing are described in section 4. The graph of the pressure window design process is shown in Figure 7.

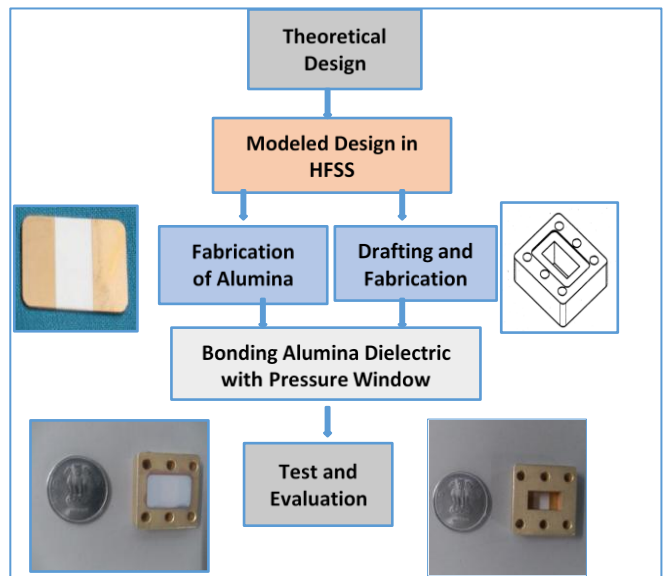


**Figure 7:** Flow graph of pressure window design process

### 4. Test and Evaluation of the WR-51 Waveguide Pressure Windows

The detailed test flow for the Ka-band WR-51 waveguide pressure windows is shown in section 4.1. On the other hand, the test plan details and the test result details for such windows are shown in sections 4.2.

#### 4.1 WR-51 Waveguide Pressure Window Test Flow

After fabrication of pressure window detailed test and qualification is carried out. A flow chart is shown in Figure 8 describing the sequence of tests carried out on each pressure window.

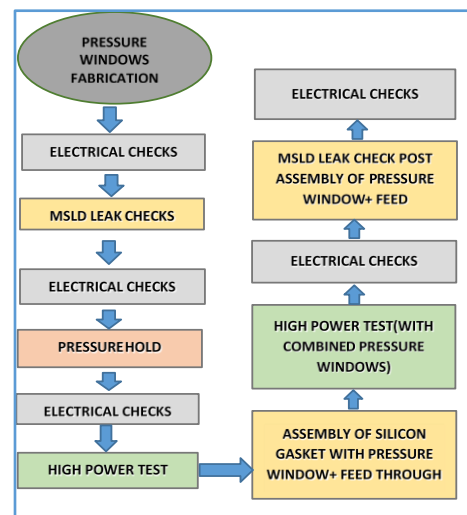


**Figure 8:** Flow graph of test and qualification of pressure window

After carrying out high power RF test in ambient conditions, pressure windows are connected to feed through. As hot redundancy, two pressure windows are connected back and to reduce the leak rate and for good arresting of RF leakage from the flange joints, silicon gaskets are used on both sides of the pressure window as shown in the Figure 9. Pressure window and feed-through is then subjected to high



power RF testing in vacuum environment. Feed-throughs then connected to thermal-vacuum chamber's flange as shown in Figure 10.

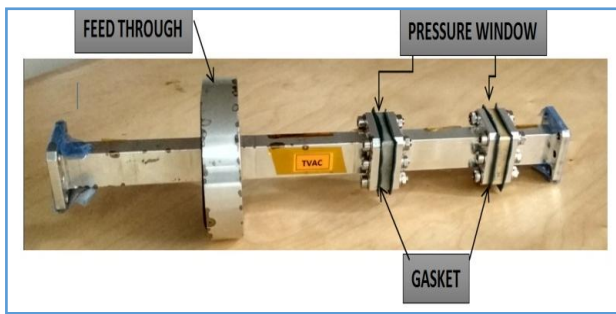
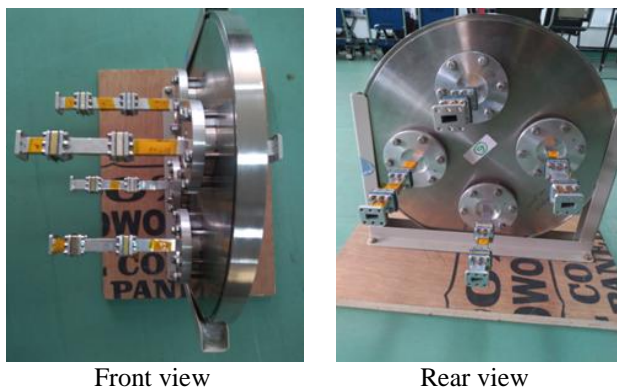


Figure 9: Pressure window connected back to back with silicon gasket to feed-through



Front view

Rear view

Figure 10: WR-51 waveguide pressure windows are connected to chamber's flange that is used in Thermal-vacuum chamber

#### 4.2 Detailed Test Results

The following tests were carried out for all the ten numbers of indigenously developed Ka-band WR-51 Pressure Windows:

- 1) Initial Electrical checks
- 2) MSLD leak checks
- 3) Pressure hold checks
- 4) High power RF test at Ambient Conditions
- 5) High power RF test at Thermal Vacuum Conditions
- 6) Final Electrical checks

##### 4.2.1 WR-51 Waveguide Pressure Window's Initial Electrical Checks

As initial electrical checks (also called passive checks), the plots of the S-parameters (namely,  $S_{11}$ ,  $S_{12}$ ,  $S_{21}$  and  $S_{22}$ ) [7] of all the WR-51 pressure windows were measured on Vector Network Analyzer (VNA). In order to measure the S-parameters of each pressure window on VNA [8], the selected pressure window was connected with a pair of WR-51 waveguide to coaxial adaptors and the entire pressure window and adaptor-pair assembly was connected to both the ports of the VNA. Hence, to compute the insertion loss due to pressure window alone, one has to subtract the insertion loss of the waveguide to coaxial adaptor-pair from the measured S-parameter ( $S_{11}$  or  $S_{11}$ ) values of the entire window-adaptor assembly. The insertion losses (maximum values) computed in this way for one set of pressure windows (i.e., PW-1 and PW-2) are shown in Table 4 along

with the measured values of their return losses (minimum values).

Table 4: Insertion loss and return loss values during initial electrical checks

Pressure window ID No.	Pressure Window Serial No.	Maximum Insertion Loss ( $S_{21}/S_{12}$ ) in dB	Minimum Return Loss ( $S_{11}/S_{22}$ ) in dB
PW 1	E8182-4	0.23	17.3
PW 2	KA-01	0.26	18.7

The S-parameter plots on VNA showing insertion loss and return loss variations over the operating frequency range of 19.5 GHz to 21 GHz for PW-1 and PW-2 WR-51 waveguide pressure windows along with WR-51 waveguide to coaxial adaptor-pair are shown in Figures 11 and 12. On the other hand, the S-parameter plots on VNA showing insertion loss and return loss variation over the same frequency band for the WR-51 waveguide to coaxial adaptor pair alone is shown in Figure 13.

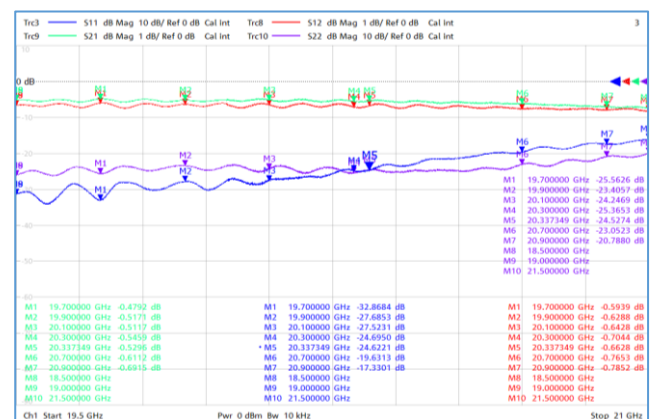


Figure 11: S-parameter plots of WR-51 Ka-band waveguide pressure window-1 (PW-1) and WR-51 waveguide to coaxial adaptor-pair assembly

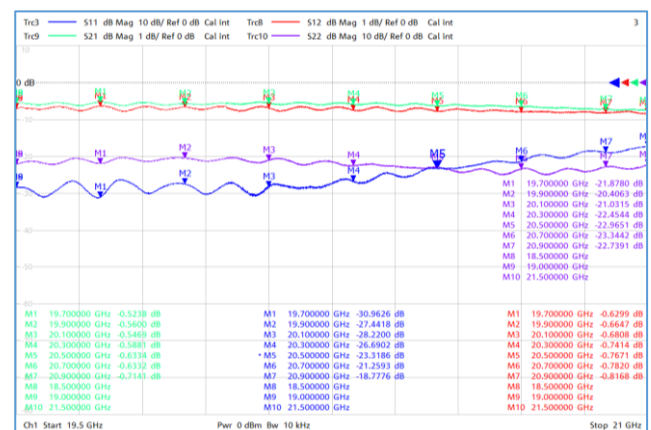


Figure 12: S-parameter plots of WR-51 Ka-band waveguide pressure window-2 (PW-2) and WR-51 waveguide to coaxial adaptor-pair assembly

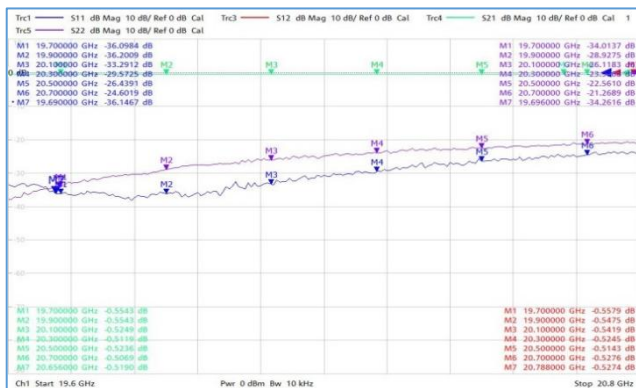


Figure 13: S-parameter plots of WR-51 waveguide to coaxial adaptor-pair

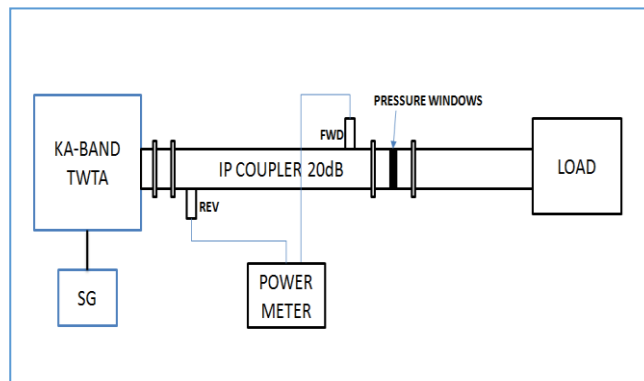


Figure 14: High power RF test setup in ambient condition for testing pressure window

4.2.2 WR-51 Waveguide Pressure Window’s MSLD leak checks

These pressure windows are tested for leak rate using Mass Spectrometer Leak Detector (MSLD) and the test results are shown in Table 5. Achieved leak rate is better than the target specification.

Table 5: MSLD Leak rate for the WR-51 waveguide pressure windows

Serial.No	Leak Rate
PW-1	1x10 <sup>-9</sup> tor.litre/sec
PW-2	1x10 <sup>-9</sup> tor.litre/sec

4.2.3 WR-51 Waveguide Pressure Windows Pressure hold checks

These pressure windows are kept in pressure hold of 2 Atmosphere for about 24 Hrs. The test results are shown in Table 6. It is meeting the targeted specification.

Table 6 : Pressure hold test results

Serial No.	Duration	Pressure hold
PW-1	24 Hrs	2 Atmosphere
PW-2	24 Hrs	2 Atmosphere

4.2.4 WR-51 Waveguide Pressure Windows High power RF test at Ambient Conditions

High power RF testing is carried out for Pressure windows by making the test setup shown in figure. Each pressure window is subjected to 200 Watt high power level for about 4 Hours in ambient conditions. In the test setup, instruments like Amplifier, Power meter, signal generator, waveguide coupler, waveguide load are used. A 20 dB coupler and power meter are used for monitoring the power level. A thermal logger is used for monitoring the temperatures. Travelling wave tube amplifier(TWTA)[9] is used for generating High-power RF signals. Waveguide Load is used to terminate the high-power RF signals. External cooling is provided to pressure window to reduce the temperatures at higher power levels. Using these instruments and waveguide components, high power RF testing is carried out in ambient conditions and the detailed test results are tabulated in Table 7.

Table 7: PW-1 High Power RF test results

TWTA DISPLAY in Watt	Power Measured in COUPLER in dBm		Temperature sensor readings in DegC		
			PW TOP	PWBOTTOM	Load
FWD	FWD	REV	T1	T2	T3
55	47.02	36.96	43.1	41.8	31.7
102	50.01	39.27	58.9	55.9	37.5
131	51.16	40.02	75.8	71.6	43.2
* External Cooling Provided to Pressure window					
155	51.78	40.87	37.7	36.9	28.9
207	53	40.31	38.9	38.9	28.6

Table 8: PW-2 High Power RF test results

TWTA DISPLAY in Watt	Power Measured in COUPLER in dBm		Temperature sensor readings in DegC		
			PW TOP	PW BOTTOM	Load
FWD	FWD	REV	T1	T2	T3
57	47.13	31.9	45.4	41.7	30.4
103	50.02	35.19	62	52.4	34.7
133	51.31	36.5	75	60.6	38.6
* External Cooling Provided to Pressure window					
160	51.71	35.94	46.5	42.6	34.6
202	52.97	38.42	54.2	49.2	38.9

4.2.5 WR-51 Waveguide Pressure Window’s High power RF Test at ThermoVacuum Conditions

Pressure windows are used in Thermovacuum chambers to isolate the vacuum environment from ambient conditions, hence these pressure windows have to be tested in Vacuum conditions as part of qualification. The test profile for the Thermal vacuum conditions is shown in the figure below

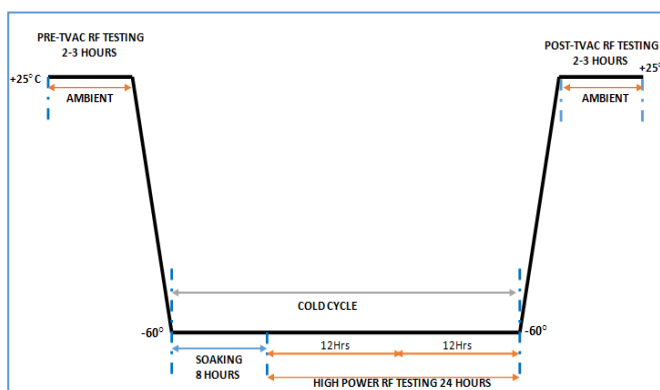


Figure 15: Thermal-vacuum test profile for pressure window qualification

High power RF testing in Thermovacuum chamber is carried out using the setup shown in figure 16. Here RF testing is done at Ambient and cold cycles by varying the temperature from -60 Deg C to +25 Deg C.

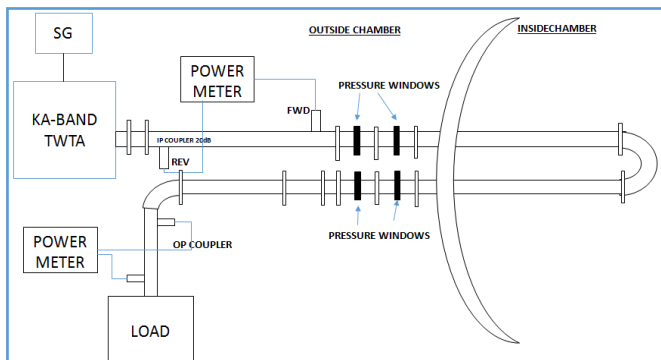


Figure 16: High power RF test setup in ambient condition for testing pressure window

Similar measurement instruments that are used in high power testing in ambient conditions are taken for this testing. Using these instruments and waveguide components [10] high power RF testing is carried out in vacuum conditions at power level of 230Watt for the duration provided in the Thermovacuum profile. The detailed test results are tabulated below. Due to increase in power level there is an increase in temperature, which reflects in changes in material properties and in turn the reflected power is varied. Reflected power variation due to increase in power level is also shown in Figure 17

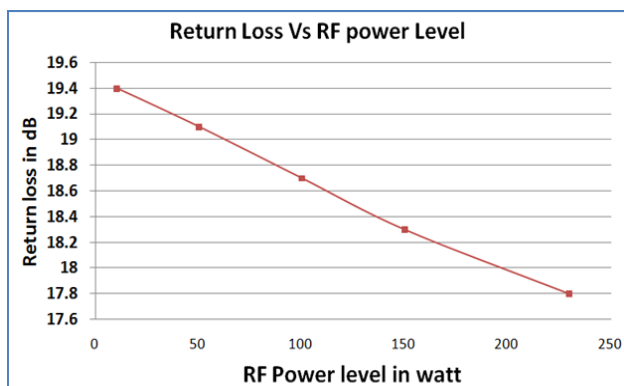


Figure 17: Return Loss variation at various RF power levels

Table 9: High power RF Test results during Cold cycle

High power RF Test results during Cold cycle			
Power level In Watt	Duration	PW1 temperature in DegC	PW2 temperature in DegC
10	10 min	28.5	28.8
50	10 min	30.3	31.9
100	10 min	32.4	35.5
200	10 min	37.3	40.3
230	12Hrs	39.4	43.4

4.2.6 WR-51 Waveguide Pressure Window’s final electrical checks

After completion of all the tests, final electrical checks are carried out and the performance is evaluated. The final S-parameter plots for the combination of back to back pressure window, feed through, silicon gasket and waveguide to coaxial adaptor pair are shown in Figure 18. On the

otherhand, the S-parameter plots for the pair of adaptors are shown in Figure 19. From these plots, the final maximum insertion loss (adaptor pair loss = 0.4 dB, feed through loss= 0.15 dB) of the individual pressure window and the final minimum return loss of the entire assembly was computed and shown in Table 10 along with their initial measured values (measured during initial electrical check) and specified/target values.

Table 10: Insertion loss and return loss values

Parameters	Final Measured values (in dB)	Initial Measured values (I ndB)	Specified values (in dB)
Maximum Insertion Loss ( $S_{21}/S_{12}$ ) of the individual pressure	0.24	0.26	$\leq 0.4$
Minimum Return Loss ( $S_{11}/S_{22}$ ) of the assembly	17.8	17.3	$\geq 15$

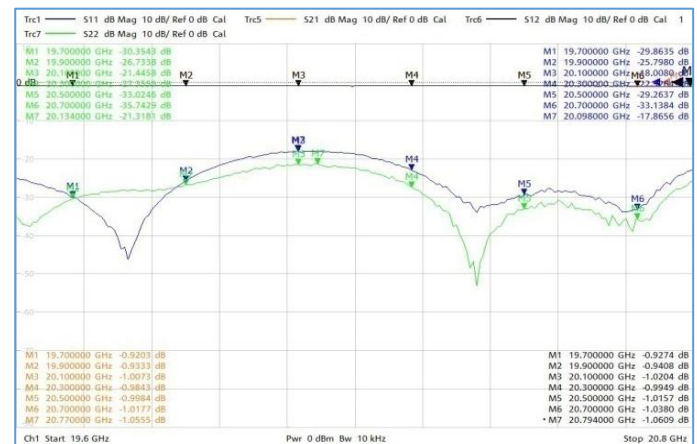


Figure 18: S-parameter plots of WR-51 waveguide to coaxial adaptor-pair

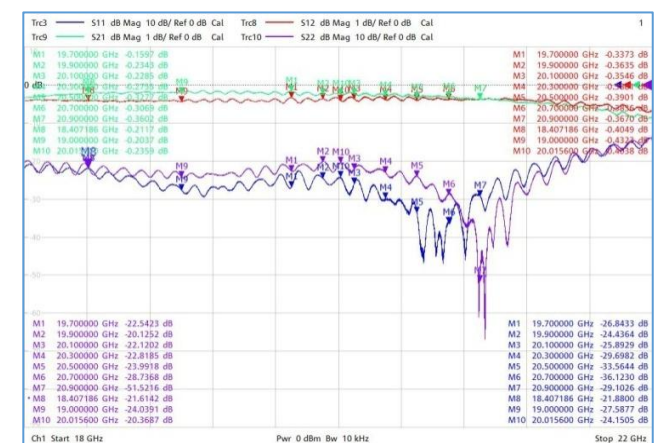


Figure 19: S-parameter plots of final assembly

5. Conclusion

Waveguide high power pressure windows have been designed, realised, tested and used for satellite testing applications. Theoretical equations are studied and the equations are coded in MATLAB and after obtaining the design parameters, simulations are carried out in HFSS. Post fabrication of waveguide pressure windows, detailed test and qualification is carried out. The Comparison of test results



obtained from HFSS Simulation of waveguide pressure windows and the realized waveguide pressure windows are found to be in good match. This developmental work has resulted in large savings in FE and in accomplishing realisation of high power high frequency waveguide within short turnaround time.

## 6. Acknowledgment

The authors are thankful to the Deputy Director, ICA, Shri Ramanagouda V Nadagouda, for their constant encouragement and motivation for writing this paper. Authors are thankful to various groups involved in realization of the pressure windows. Finally, the authors are very much grateful to the high power RF team (at high power RF lab/ISITE campus) and the payload checkout team for their extended support to carry out the test and evaluation of these indigenously developed pressure windows.

## 7. Disclosure Statement

No potential conflict of interest was reported by the authors

## References

- [1] George L. Ragan, "Microwave Transmission Circuits" McGraw Hill, London (1948).
- [2] Latha Christie and Sritama Dutta "Design and Comparison of Waveguide Windows", Procedia Comput. Sci., vol. 93, pp. 243-250, Sep. 2016.
- [3] Nathan Marcuvitz, "Waveguide Handbook", New York: McGraw Hill, 1951.
- [4] Caspers, Fritz, "RF Engineering Basic Concepts: S-parameters", 2012.
- [5] Imamou Dawut, "Application of MATLAB in Solving Function and Derivation [J]". Mathematics Learning and Research, 2012(15), pp. 11-12.
- [6] H. Srikanth Kamath, Rachit Arora, Vriti Agarwal, "Studying the Characteristics of Rectangular Waveguide using HFSS". International Journal of Computer Application, 2015; 118(1).
- [7] D. M. Pozar, "Microwave Engineering", John Wiley & Sons, 4th edition, 2011.
- [8] C. D. M. Ambatali, "Implementation of an oscilloscope vector network analyzer for teaching s-parameter measurements", Conference paper, 2018 IEEE Region 10 Humanitarian Technology Conference (R10-HTC), pp. 1-6, Dec 2018.
- [9] RJ Barker (Ed) & Edl Schamiloglu (Ed), "High-Power Microwave Sources and Technologies", Wiley-IEEE Press, June 2001.
- [10] RE. Collin, "Foundation for Microwave Engineering, 2<sup>nd</sup> Edition, New York, McGraw Hills, 1992.

## Author Profile



**Karri V R Dinesh Kumar Reddy.** He is a scientist at U R Rao Satellite Centre. He joined ISRO in the year 2016. His research interest includes the Design of Pressure Windows, Ring Resonators, Waveguide transitions, Microwave & RF Communication systems. Presently he is working as a Test Engineer in GEOSAT RF & Payload Checkout Division. **Email:** [dineshk@urisc.gov.in](mailto:dineshk@urisc.gov.in)



**Md. Tosicul Wara.** He is a scientist at UR Rao Satellite Centre. He joined ISRO in 1993. Presently he is the head of GEOSAT RF & Payload Checkout Division-1 (GRCD-1) of Spacecraft Checkout Group at U R Rao Satellite Centre, Bangalore. His field of interest includes Satellite Communication, Global Navigational Satellite System (GNSS), and Microwave Measurement & Instrumentations. He is a fellow of the Institution of Electronics & Telecommunication Engineers (IETE). **Email:** [tosi@urisc.gov.in](mailto:tosi@urisc.gov.in)



**Shaji V. Sebastian** He is a Scientist at ISRO Satellite Centre. He joined ISRO in the year 1990. Presently he is the head of IRS RF & Payload Checkout Division-1 (IRCD-1) of Spacecraft Checkout Group at U R Rao Satellite Centre, Bangalore. His main research interest includes RF passive components, like Antennas, Filters etc. **Email:** [sebas@urisc.gov.in](mailto:sebas@urisc.gov.in)



**T. Ramesh Babu Reddy**-He is a scientist at U R Rao Satellite Centre. He joined ISRO in the year 1997. His research interest includes RF communication systems, DDS-based Frequency Synthesizers, Digital & analog Up/Down Converters, TTC RF Ground Transmitters. Presently he is the Section head in GEOSAT RF & Payload Checkout Division (GRCD). **Email:** [trbabu@urisc.gov.in](mailto:trbabu@urisc.gov.in)



**Kraleti Chandrasekharam.** He is a scientist at UR Rao Satellite Centre. He joined ISRO in 1997. His field of interest includes Satellite Communication, Global Navigational Satellite System (GNSS), and Design and development of Analog & digital demodulators. He is a member of Astronautical Society of India (ASI). **Email:** [kchandru@urisc.gov.in](mailto:kchandru@urisc.gov.in)



**Usha Bhandiwad.** She is a scientist at UR Rao Satellite Centre (URSC) and presently she is the Group Director of Spacecraft Checkout Group (SCG) of URSC. She received B.E. degree in Electronics and Communication Engineering from Karnataka University, Dharwad. Presently her work areas include design, development and realization of simulators and providing automation for spacecraft testing. **Email:** [usharb@urisc.gov.in](mailto:usharb@urisc.gov.in)